

4 **Running title:** Low WNK4 expression promotes gastric cancer proliferation

5
6 **Downregulation of WNK4 expression facilitates the proliferation of gastric cancer cells via**
7 **activation of the STAT3 signaling pathway**

8
9 Miao Li^{1,#}, Xiaoyan Shao^{2,#}, Qiqi Ning³, Rongrong Sun², Rantian Li², Yanhua Liu², Yuan Yuan^{2,*},
10 Youwei Zhang^{1,2,*}

11
12 ¹Jinzhou Medical University Postgraduate Training Base (Xuzhou Central Hospital), Jinzhou,
13 China; ²Department of Medical Oncology, Xuzhou Central Hospital, Xuzhou, China; ³Department
14 of Molecular Microbiology and Immunology, University of Southern California Keck School of
15 Medicine, Los Angeles, California, United States

16
17 *Correspondence: yuan yuan87303@163.com, zhangyw@njmu.edu.cn

18
19 #Contributed equally to this work.

20
21 **Received February 20, 2024 / Accepted May 1, 2024**

22
23 WNK lysine deficient protein kinase 4 (WNK4) has been shown to be significantly associated with
24 cancer progression. Nevertheless, its involvement in gastric cancer (GC) is unclear. The objective of
25 this work was to investigate the WNK4's regulatory mechanism in GC. Quantitative RT-PCR and
26 immunoblots revealed that WNK4 expression was downregulated in GC and that low expression of
27 WNK4 was strongly linked to poor prognosis. Functional assays including cell counting kit-8 assay
28 and colony formation assay demonstrated that overexpression of WNK4 led to limited tumor
29 proliferation both *in vitro* and *in vivo*, while the WNK4 reduction yielded to the opposite results.
30 Gene Set Enrichment Analysis (GSEA) indicated a potential association between WNK4 and the
31 signal transducer and activator of transcription (STAT3). WNK4 suppressed the phosphorylation of
32 signal transducer and activator of transcription 3 (p-STAT3) in GC cells. The inhibition of the
33 STAT3 pathway with Stattic reversed growth and proliferation induced by WNK4 knockdown in
34 GC cells. These findings provide new insights for identifying key therapeutic targets for GC in the
35 future.

36
37 **Key words:** WNK4; gastric cancer; proliferation; tumorigenesis; STAT3

38
39
40 According to the latest GLOBOCAN 2020 data, GC ranked fifth globally in terms of incidence of
41 malignant tumors [1]. GC patients were typically diagnosed at intermediate or advanced stages,

42 resulting in missed opportunities for optimal surgical intervention and unfavorable prognoses.
43 Despite the availability of comprehensive treatment approaches such as palliative surgery,
44 radiotherapy, chemotherapy etc., their efficacy remained unsatisfactory [2-4]. Particularly when
45 compared to the progress made in targeted therapy for advanced lung adenocarcinoma cases over
46 recent years, patients with advanced GC experienced a lagging prognosis. This can be primarily
47 attributed to the high heterogeneity of GC and its yet incompletely understood pathogenesis.
48 Although targeted therapy and immunotherapy had introduced new strategies for treating GC,
49 overall survival rates for advanced cases had not significantly improved [5, 6]. Therefore,
50 elucidating the mechanisms behind GC is crucial for optimizing treatment regimens.

51 STAT3 is a multifunctional molecule engaged in signal transduction and transcriptional activation,
52 playing crucial roles in inflammation, metabolism, and tumorigenesis [7, 8]. Previous studies had
53 shown that the IL-6/IL-8/IL-11-mediated JAK-STAT pathway promotes GC growth and invasion
54 [9-11]. Additionally, *Helicobacter pylori* (*H. pylori*) infection activated STAT3 which binds directly
55 to the TMEFF2 gene promoter region leading to its down-regulation. Simultaneously, TMEFF2
56 negatively regulated STAT3 activation through SHP-1, thereby promoting GC progression through
57 this feedback loop [12]. Moreover, SPI1 enhanced the malignant phenotype of GC through
58 activating the IL6/JAK2/STAT3 signaling pathway [13]. Targeting the STAT3 pathway holds
59 significant potential for innovative treatment strategies against GC. Costa et al. [14] discovered that
60 silencing WNK2 kinase activates c-Jun N-terminal kinase (JNK), thus promoting glioma
61 development. Given the close association between JNK kinase and STAT3 signaling pathway, it
62 was presumed that WNK2 acted via activating the STAT3 pathway. Consequently, WNK might
63 played a pivotal role in tumorigenesis.

64 With-no-lysine (WNK) kinases, a class of serine/threonine protein kinases, were implicated in
65 various cancer-related signaling cascades, highlighting their multifaceted roles [15, 16]. WNK1 is
66 implicated in adverse prognosis in hepatocellular carcinoma (HCC) and colorectal cancer (CRC)
67 [17, 18]. Conversely, silencing of WNK2 correlated with tumor recurrence and inferior overall
68 survival (OS) in HCC, accompanied by invasion of tumor-associated macrophages [19]. WNK3
69 potentiates invasiveness in a manner that induces glioma epithelial-to-mesenchymal transition in

70 hypoxic conditions [20]. Up-regulation of WNK4 enhanced medulloblastoma cell proliferation and
71 confers resistance to cisplatin treatment, contributing to poor prognosis [21]. Nevertheless, WNK4
72 's involvement in GC remains to be explored.

73 We investigated the influence and manifestation of WNK4 in GC cells and noted that WNK4
74 operates as a cancer inhibitor in GC. Moreover, downregulation of WNK4 expression augmented
75 STAT3 pathway activity in GC cells, while inhibition of the STAT3 pathway with Stattic reversed
76 growth and proliferation induced by WNK4 knockdown in GC cells. These findings suggested that
77 reduced WNK4 expression promoted the growth of GC cells through activation of the STAT3
78 signaling pathway, thereby providing a promising direction for GC therapy.

79

80 **Materials and methods**

81 **Data collection and analysis.** In previous work, one hundred gastric cancer tissues and paired
82 normal tissue specimens were retrieved from our specimen bank of Xuzhou Central Hospital were
83 mobilized to detect mutations in WNK family genes by targeted sequencing. It was carried out
84 according to the ethical standards approved by the Ethics Committee of the hospital. To examine
85 the level of WNK4 in GC, we utilized the Box plot function available in the Gene Expression
86 Profiling Interactive Analysis (GEPIA) database (<http://gepia.cancer-pku.cn/index.html>).
87 Furthermore, the University of ALabama at birmingham CANcer (UALCAN) database platform
88 (<http://ualcan.path.uab.edu/index.html>) was utilized to investigate changes in gene expression across
89 various grades and stages of GC. The immunohistochemistry findings from Human Protein Atlas
90 (HPA) database. (<https://www.proteinatlas.org>) provided valuable insights into the expression
91 patterns of WNK4 in various tissues. To explore the prediction value of WNK4 expression on GC
92 survival, we downloaded the normalized mRNA expression profiles of GC cohort (N=410) and its
93 corresponding survival information from <https://xena.ucsc.edu/>. To carry out survival analysis, the
94 'survminer' package was applied. In order to identify the most significant survival differences, the
95 `surv_cutpoint` function, with a `minprop` value of 0.1, was utilized to determine the optimal threshold
96 for grouping.

97 **Cell lines and cell culture.** For this study, we obtained GC cell lines (AGS , HGC27 , MKN28 ,
98 MKN45 , and NCIN87) and the human gastric epithelium cell line (GES-1) from the Cell Resource
99 Center at the Shanghai Institutes for Biological Sciences, Chinese Academy. Culturing of the cells
100 involved the RPMI1640 (Biosharp, #BL303A) supplemented with 10% fetal bovine serum (Gibco,
101 #16000-044) and 1% penicillin/streptomycin (Solarbio, #P1400-100). The cells were incubated at
102 37 °C with a CO₂ concentration of 5% to maintain the optimal growth conditions.

103 **Lentivirus infection.** Overexpressing and shRNA lentiviral WNK4 vectors were constructed by
104 Shanghai GenePharma Co (China). shRNAs for WNK4-1, WNK4-2 or WNK4-3 were inserted into
105 the pLKO.1 plasmid (Supplementary Table S1). To overexpress WNK4, coding sequences were
106 inserted into the pLVX-Puro plasmids. In 6-well culture plates, the AGS or MKN45 cells were
107 seeded individually during their logarithmic growth phase at a density of 5×10^5 cells/well.
108 Following this, the cells were lentivirally transfected until reaching approximately 60% confluency.
109 To carry out subsequent experiments, the cells were collected after 72 h by adding a blend of 5 μ l
110 lentivirus and 1 μ l polybrene (5 μ g/ μ l) to each well.

111 **Western blotting analysis.** Protein extraction was conducted using the rapid lysate cell kit
112 (Beyotime, #P0013). The protein concentration was determined with the BCA Protein Assay kit
113 (Beyotime, #P0012). The protein lysate separated by 10% SDS-PAGE was transferred onto the NC
114 membrane (Millipore, #HATF00010). We blocked the membranes with 5% skimmed milk.
115 Subsequently, they were incubated overnight at 4 °C with following primary antibodies: WNK4
116 (1:1000, Cell Signaling Technology (CST), #5713), STAT3 (1:1000, Abcam, #AB68153),
117 p-STAT3 (1:1000, Abcam, #AB267373), GAPDH (1:2000, CST, #5174). The blots were further
118 treated with an additional incubation period for 1 h with HRP-labelled anti-mouse (1:1000,
119 Beyotime, #A0216) or anti-rabbit (1:1000, Beyotime, #A0208). Finally, enhanced visualization of
120 target protein bands.

121 **Cell counting Kit-8 (CCK-8) assay.** In order to evaluate cell proliferation, we utilized the CCK-8
122 assay. In concrete terms, cells were cultured in 96-well plates with an initial density of 3×10^3
123 cells/well at 37 °C in a 5% CO₂ environment for an overnight duration. Subsequently, the

124 supernatant was removed, and each well received 10 μ l of CCK-8 reagent (Signalway Antibody
125 (SAB), #CP002) at: 0, 12, 24, 48, and 72 h. Incubation of the plates was then carried out under
126 light-protected for one hour. Eventually, the absorbance at 450 nm was conducted.

127 **Colony formation assay.** Inoculated 1×10^3 cells/well in a culture plate routinely. The plates were
128 stored in an incubator at 37 °C for a total duration of 21 days. Removed liquid above the cells was
129 eliminated, and the cells were rinsed twice. Cells were immobilized using a solution of 4%
130 paraformaldehyde for a period of 15 min. Afterwards, staining was applied with 0.1% crystal violet
131 solution for 10 min. Lastly, the staining solution was slowly washed off with running water, and the
132 plates were left to dry at room temperature before observing the colonies.

133 **Real-time quantitative PCR (qPCR).** Extraction of total RNA was carried out with TRIzol
134 reagent (Invitrogen, #1596-026). Following this, a reverse transcription kit (Yesen, #11123ES60)
135 was used for synthesizing cDNAs. The SYBR Green PCR kit (Yesen, #11202ES03/08/60) was
136 utilized for conducting real-time quantitative PCR analysis. A PCR detector (Heal Force) was
137 employed under specific conditions: a denaturation step, lasting for 5 min at 95 °C, which was
138 followed by a series of 40 cycles. Each cycle comprises 10 s of denaturation and 30 s of
139 annealing/extension at the corresponding temperature. Each reaction consisted of 10ng of sample
140 cDNA and HPLC-grade water to make up a final volume of 20 μ l. GAPDH as an internal control to
141 ensure accuracy. The $2^{-\Delta\Delta CT}$ approach was employed for the computation of the relative expression
142 of WNK4. The primer sequences utilized are presented in Table 1.

143 **Nude mice xenograft model.** We obtained four-to six-week-old male BALB/c-nude mice from
144 Xuzhou Medical University Laboratory Animal Center. Allocated randomly them into the oeWNK4
145 group and Vector group (n=6/group). Nude mouse xenograft models were established by
146 subcutaneously injecting 100 μ l (5×10^6 cells) of AGS cells transfected with either the WNK4
147 vector or the empty vector. During our study, tumor growth indicators, including the measurements
148 of tumor length (L) and width (W), were assessed at intervals of three days. Tumor volume was
149 calculated as $\frac{1}{2} \times (L \times W^2)$. After 5 weeks, euthanasia of the mice was performed through cervical
150 dislocation. The resulting tumors were excised, weighed, and subsequently preserved at -80 °C. All

151 of the animal experimental protocols were received approval from the Experimental Animal Ethics
152 Committee of Xuzhou Medical University.

153 **Immunofluorescence (IF) staining.** The subcutaneous tumor tissues obtained from nude mice
154 were fixed and embedded for dehydration. Afterwards, the specimens were sectioned into a
155 thickness of 5 μm and mounted on glass slides. The sections underwent an overnight incubation at
156 4 °C with a rabbit monoclonal antibody against Ki67 (dilution of 1:200; Abcam; #AB243878).
157 Subsequently, they were treated with Alexa Fluor488-conjugated IgG (dilution of 1:500; Beyotime;
158 #A0423) at a temperature of 25 °C for 1 h. DAPI staining was performed followed by image
159 acquisition with confocal microscopy. Fluorescence intensity was finally analyzed by using Image
160 J.

161 **Gene Set Enrichment Analysis (GSEA).** To perform gene set enrichment analysis, we selected
162 GC with the highest expression of WNK4 ($> Q3$) or the lowest expression of WNK4 ($< Q1$) from
163 the TCGA database to identify the signaling pathways primarily linked to WNK4 expression. Using
164 the MSigDB hallmarked gene set collection, GSEA was conducted through the JAVA program
165 available at (<http://software.broadinstitute.org/gsea/index.jsp>). This analysis involved ranking the
166 genes based on their enrichment score, ranging from the most positive to the most negative. By
167 doing so allowed us to assess the general correlation between gene sets and WNK4 expression. We
168 conducted 1,000 arbitrary permutations on a sample and set the significance threshold for the
169 p-value of the Normal distribution to be < 0.05 . If a cluster of genes exhibited a positive enrichment
170 score, most of its constituents displayed elevated expression levels in conjunction with decreased
171 WNK4 expression, therefore labeling the cluster as "enriched".

172 **Statistical analysis.** Mean \pm SD of three or more independent experiments were employed for the
173 presentation of all data after performing statistical analysis through SPSS 19.0 and GraphPad Prism
174 9.0. To compare gene expression among samples at various stages and grades, we utilized the
175 Kruskal-Wallis's test, whereas a one-way ANOVA test was employed to perform multiple
176 comparisons. The correlations from WNK4 to genes within JAK-STAT pathway were computed by
177 Pearson Correlation Coefficient. The notable differences between the two groups was conducted by
178 Student's t-test. $P < 0.05$ was considered statistically significant.

Accepted manuscript

181 **Results**

182 **WNK4 was downregulated in GC and associated with a poor prognosis.** Initially, we performed
183 targeted sequencing of one hundred gastric cancer tissues and paired normal tissue specimens in
184 order to detect mutations of WNK family genes in gastric cancer, and found that WNK1, WNK2,
185 WNK3, and WNK4 were mutated in gastric cancer tissues, with WNK4 having a significantly
186 higher mutation rate of 8% compared with other members (Figure 1A). Therefore, we focused on
187 the relationship between WNK4 and gastric cancer. We employed an online application based on
188 analysis of the TCGA database to compare mRNA levels of WNK4 between GCs and normal
189 tissues. Our findings revealed a statistically significant downregulation of WNK4 mRNA
190 expression in GC tissue (Supplementary Figure S1A). We characterized WNK4 protein expression
191 in the HPA database. Immunohistochemical analysis with antibody HPA016500. Remarkably,
192 reduced levels of WNK4 were observed in GC tissues compared to moderate to high levels found in
193 normal gastric tissue samples (Supplementary Figure S1B). There was a gradual decrease in WNK4
194 mRNA levels with increasing grade of GC (Supplementary Figure S1C). Although no noticeable
195 variances were observed among different stages of GC (Stage I-IV), there was a trend towards
196 reduced WKN4 mRNA expression as the disease progressed (Supplementary Figure S1D). In
197 addition, we validated the results of bioinformatics analysis through WB and qPCR experiments.
198 The data revealed that WNK4 exhibited significantly lower mRNA expression levels (Figure 1B)
199 and protein levels (Figure 1C) in GC cell lines compared to the GES-1 cell line. The TCGA
200 standardized GC cohort (N=410) mRNA expression patterns and their corresponding survival
201 information were downloaded to investigate the predictive value of WNK4 expression for GC
202 survival. Patients with an elevated WNK4 expression had a prolonged overall survival (OS), as
203 confirmed by univariate survival analysis. (Supplementary Figure S1E). Combined, above results
204 suggest that WNK4 affected the progression and prognosis on GC.

205 **Overexpression of WNK4 in GC cells inhibited proliferation *in vitro* and *in vivo*.** Among the
206 five GC cell lines, AGS cell line was with the lowest endogenous WNK4 expression. We then
207 investigated the impact of WNK4 on GC cell biology behavior by transfecting AGS cells with
208 WNK4 slow retroviruses (AGS/ oe - WNK4). The results obtained from RT-PCR and WB analysis

209 demonstrated a high transfection efficiency (Figures 2A, 2B). Besides, it was observed that
210 overexpression of WNK4 notably restrained the proliferation and colony-forming ability of AGS
211 cells through CCK8 assay and colony-forming assay (Figures 2C, 2D). To further validate these
212 findings, we established an *in vivo* subcutaneous xenograft model using either AGS/oe-WNK4 or
213 normal control AGS cells (Vector), which unequivocally confirmed that WNK4 overexpression
214 effectively inhibited the tumorigenic potential of AGS cells (Figures 2E, 2G). Furthermore,
215 immunofluorescence experiments conducted on paraffin sections showed a remarkable reduction in
216 the Ki-67 index of subcutaneous tumors formed by AGS/oe-WNK4 cells compared to those formed
217 by AGS/Vector cells as depicted in Figures 2H and 2I. Thus, our study provided compelling
218 evidence supporting the inhibitory role of WNK4 in GC.

219 **Knockdown of WNK4 resulted in GC cell progression.** WNK4 expression was greatest in MKN
220 45 cells among the five GC cell lines, thereby we down-regulated WNK4 expression in the MKN
221 45 cell line. First, the efficiency of knockdown was assessed by utilizing RT-PCR and Western
222 blotting techniques. (Figures 3A, 3B). Subsequently, shWNK4-1 and shWNK4-2 exhibiting
223 superior transfection efficiency were chosen for subsequent experiments. As anticipated, WNK4
224 knockdown did result in promotion of cell proliferation and colony formation (Figures 3C, 3D).

225 **The closely association between WNK4 expression and the Jak-STAT3 signaling pathway.**

226 WNK4 acted as a tumor suppressor gene in GC through the aforementioned experimental results.
227 Based on the gene expression profiles of GC extracted from TCGA database, we applied GSEA to
228 explore the potential signaling pathways associated with WNK4 expression. The results showed
229 that a significant association between WNK4 and the IL6 Jak STAT3 signaling pathway, indicating
230 that low WNK4 expression could lead to activation of IL6 Jak STAT3 signaling pathway (NES=1.7,
231 $p=0.0077$, Figure 4A). Furthermore, we extracted the key genes in the JAK-STAT3 pathway from
232 the KEGG database, and calculated the expression correlation with WNK4. The results showed that
233 most key genes in the JAK-STAT3 pathway showed a significant negative correlation with WNK,
234 including JAK1/JAK2/JAK3, STAT1/ STAT2/ STAT3/ STAT4/ STAT5A (Figure 4B). These
235 results indicated the closely association between WNK4 expression and the Jak-STAT3 signaling
236 pathway.

237 **Knockdown of WNK4 activated STAT3 signaling pathway in GC cells.** STAT3 was a
238 multifunctional molecule involved in signal transduction and transcriptional activation in biological
239 processes including inflammation, metabolism, and tumorigenesis [7, 8]. STAT 3 signaling
240 pathway has been previously demonstrated in GC [22-25]. We revealed the correlation of WNK4
241 with the STAT 3 signaling pathway in GC for the first time. Firstly, we examined the activation of
242 STAT3 (tyrosine phosphorylation at Y705), as depicted in Figure 5A. AGS cells overexpressing
243 WNK4 exhibited a significant reduction in p-STAT3 (Y705) levels, while MKN45 cells with
244 knockdown of WNK4 showed a substantial increase in pSTAT3 (Y705) expression (Figure 5B).
245 Subsequently, we employed Stattic - a non-peptide small molecule known to selectively inhibit
246 STAT3 SH2 domain function [26]. Stattic used in this study was provided by Med Chem Express
247 (MCE, #HY-13818), and the experimental concentration of Stattic was 10 μ M. The results depicted
248 in Figure 5C demonstrated that Stattic significantly attenuated STAT3 phosphorylation in GC cells
249 exhibiting low WNK4 expression. CCK8 assay and colony forming experiment suggested that
250 blockade of the STAT3 signaling pathway promoted cell death in WNK4 knockdown MKN45 cells
251 (Figures 5D, 5E). These findings imply that the low expression of WNK4 activates the STAT3
252 signaling pathway and drives tumorigenesis in GC (Figure 5F).

253

254 **Discussion**

255 The WNK family represents a novel class of serine/threonine protein kinases [27]. The name
256 "WNK" was derived from the absence of an ATP-binding lysine residue on the second subunit of its
257 kinase domain, which distinguished it from other kinases. In WNK kinases, the beta chain of lysine
258 residues within the structural domain subunit 1 played a crucial role in mediating ATP binding and
259 phosphorylation events. Adjacent to the kinase domain lies an autoinhibitory domain that maintains
260 WNK kinase activity at a low level through autophosphorylation processes [28]. Increasing
261 evidence suggested aberrant expression of WNK in tumor tissues, implicating its involvement in
262 tumor growth, metastasis, and angiogenesis [29]. This article focused on elucidating the WNK4 in
263 gastric cancer.

264 We observed for the first time that WNK4 protein and mRNA were expressed at lower levels in GC
265 samples than those in normal tissues and cells, as determined using a large public database. To
266 validate these findings, Western blotting and RT-PCR were employed to determine WNK4
267 expression in GC cells and normal human gastric epithelial cells. The results demonstrated a
268 substantial decrease in WNK4 expression within GC cells in contrast to GES-1, which corroborated
269 data from TCGA and HPA databases. Moreover, analysis of TCGA database revealed a correlation
270 between low WNK4 expression and advanced tumor stage, grade, as well as poor clinical outcome.
271 AGS cells with relatively low endogenous WNK4 expression were selected for overexpression
272 experiments. Our data showed that GC cells overexpressing WNK4 exhibited significantly reduced
273 proliferative capacity. Conversely, MKN45 cells with relatively high endogenous WNK4
274 expression were chosen for knockdown experiments, resulting in enhanced proliferation ability of
275 GC cells with suppressed levels of WNK4. It was noteworthy that different members within the
276 WNK family played distinct roles across various types of tumors. Previous study had reported high
277 expression levels of WNK1 in HCC, where it was related to poor prognosis [30]. Additionally,
278 research on colon cancer cell lines had shown that silencing or inhibiting WNK1 effectively
279 suppressed both *in vitro* and *in vivo* proliferation of colon cancer [31]. Downregulation of WNK1
280 expression in various breast cancer models had demonstrated a reduction in tumor migration,
281 invasion, demonstrating that targeting WNK1 could serve as a strategy for mitigating the
282 progression of invasive breast cancer [32]. Decreased expression of WNK2 had been correlated
283 with tumor recurrence and adverse OS outcomes in patients with HCC [19]. Suppression of WNK2
284 in the glioblastoma SW1088 cell line enhanced cell migration and invasion and soft agar colony
285 formation. Conversely, reintroduction of WNK2 into A172H glioblastoma cells obstructed their
286 capacity to establish clusters in soft agar and suppressed tumor development in a chick
287 chorioallantoic tumor model [33]. This evidence backed WNK2 as a potent tumor suppressor. It can
288 be seen a dual function for WNK proteins in tumorigenesis. Interestingly, in both medulloblastoma
289 and gastric cancer, STAT3 appears to be a key transcriptional regulator, while they differ in WNK4
290 expression. Up-regulation of WNK4 enhanced medulloblastoma cell proliferation and confers

291 resistance to cisplatin treatment, contributing to poor prognosis. However, as we found,
292 upregulation of WNK4 inhibited the proliferation of gastric cancer cells.

293 Next, we investigate the mechanisms of regulating GC after WNK4 knock-down. GSEA revealed a
294 negative correlation between WNK4 and the STAT3 signaling pathway. This was further validated
295 through cell experiments, where in overexpression of WNK4 led to a notable reduction in p-STAT3
296 expression in GC cells, which was substantially increased when WNK4 knockdown. Furthermore,
297 we observed that STAT3 inhibitors could counteract the effects of WNK4 knock-down on GC cells.
298 Here, we concluded that WNK4 suppression may induce GC proliferation through activation of the
299 STAT3. Hyperactivation of the STAT3 pathway had been observed in various human tumors such
300 as HCC and CRC, classifying it as an oncogene [34, 35]. RBMS1 promoted GC metastasis via
301 autocrine IL-6/JAK2/STAT3 signaling [36], the acceleration of GC cell proliferation and invasion
302 was facilitated by circBGN through the activation of the IL6/STAT3 pathway [37], and Kras or
303 BRAF mutation synergise with STAT3 activation contribute to GC progression [38]. Altogether,
304 these highlighted a strong connection between STAT3 pathway and GC.

305 We revealed a novel mechanism underlying gastric carcinogenesis. However, the specific
306 mechanisms by which reduced expression of WNK4 induced activation of the STAT3 in GC remain
307 unclear, and further investigations will be conducted to address this question.

308 Our findings not only provided deeper insights into the role of WNK4 in GC but also presented the
309 first evidence suggesting that WNK4 may function as a tumor suppressor gene. Therefore, WNK4
310 could be considered a promising new target for optimizing clinical practice.

311

312 Acknowledgments: The research was funded by the National Natural Science Foundation of China
313 (81973346) and Jiangsu Province medical key discipline project (ZDXK202237).

314

315 **Supplementary data are available in the online version of the paper.**

316

317

318 **References**

- 319 [1] SUNG H, FERLAY J, SIEGEL RL, LAVERSANNE M, SOERJOMATARAM I et al.
320 Global Cancer Statistics 2020: GLOBOCAN Estimates of Incidence and Mortality
321 Worldwide for 36 Cancers in 185 Countries. *CA Cancer J Clin* 2021; 71: 209-249.
322 <https://doi.org/10.3322/caac.21660>
- 323 [2] CATS A, JANSEN EPM, VAN GRIEKEN NCT, SIKORSKA K, LIND P et al.
324 Chemotherapy versus chemoradiotherapy after surgery and preoperative chemotherapy for
325 resectable gastric cancer (CRITICS): an international, open-label, randomised phase 3 trial.
326 *Lancet Oncol* 2018; 19: 616-628. [https://doi.org/10.1016/S1470-2045\(18\)30132-3](https://doi.org/10.1016/S1470-2045(18)30132-3)
- 327 [3] SITARZ R, SKIERUCHA M, MIELKO J, OFFERHAUS GJA, MACIEJEWSKI R et al.
328 Gastric cancer: epidemiology, prevention, classification, and treatment. *Cancer Manag Res*
329 2018; 10: 239. <https://doi.org/10.2147/CMAR.S149619>
- 330 [4] CAO Y, JIAO N, SUN T, MA Y, ZHANG X et al. CXCL11 Correlates With Antitumor
331 Immunity and an Improved Prognosis in Colon Cancer. *Front Cell Dev Biol* 2021; 9:
332 646252. <https://doi.org/10.3389/fcell.2021.646252>
- 333 [5] KIM ST, CRISTESCU R, BASS AJ, KIM KM, ODEGAARD JI et al. Comprehensive
334 molecular characterization of clinical responses to PD-1 inhibition in metastatic gastric
335 cancer. *Nat Med* 2018; 24: 1449-1458. <https://doi.org/10.1038/s41591-018-0101-z>
- 336 [6] ZENG Y, JIN RU. Molecular pathogenesis, targeted therapies, and future perspectives for
337 gastric cancer. *Semin Cancer Biol* 2022; 86: 566-582.
338 <https://doi.org/10.1016/j.semcancer.2021.12.004>
- 339 [7] GAO Q, WOLFGANG MJ, NESCHEN S, MORINO K, HORVATH TL et al. Disruption of
340 neural signal transducer and activator of transcription 3 causes obesity, diabetes, infertility,
341 and thermal dysregulation. *Proc Natl Acad Sci U S A* 2004; 101: 4661-4666.
342 <https://doi.org/10.1073/pnas.0303992101>
- 343 [8] INOUE H, OGAWA W, OZAKI M, HAGA S, MATSUMOTO M et al. Role of STAT-3 in
344 regulation of hepatic gluconeogenic genes and carbohydrate metabolism in vivo. *Nat Med*
345 2004; 10: 168-174. <https://doi.org/10.1038/nm980>
- 346 [9] OLLILA S, DOMÈNECH-MORENO E, LAAJANEN K, WONG IP, TRIPATHI S et al.
347 Stromal Lkb1 deficiency leads to gastrointestinal tumorigenesis involving the
348 IL-11-JAK/STAT3 pathway. *J Clin Invest* 2018; 128: 402-414.
349 <https://doi.org/10.1172/JCI93597>
- 350 [10] LI W, ZHANG X, WU F, ZHOU Y, BAO Z et al. Gastric cancer-derived mesenchymal
351 stromal cells trigger M2 macrophage polarization that promotes metastasis and EMT in
352 gastric cancer. *Cell Death Dis* 2019; 10: 918. <https://doi.org/10.1038/s41419-019-2131-y>
- 353 [11] SOUTTO M, CHEN Z, BHAT AA, WANG L, ZHU S et al. Activation of STAT3 signaling is
354 mediated by TFF1 silencing in gastric neoplasia. *Nat Commun* 2019; 10: 3039.
355 <https://doi.org/10.1038/s41467-019-11011-4>
- 356 [12] SUN TT, TANG JY, DU W, ZHAO HJ, ZHAO G et al. Bidirectional regulation between
357 TMEFF2 and STAT3 may contribute to Helicobacter pylori-associated gastric
358 carcinogenesis. *Int J Cancer* 2015; 136: 1053-1064. <https://doi.org/10.1002/ijc.29061>

- 359 [13] HOU G, ZUO H, SHI J, DAI D, WANG H et al. EIF4A3 induced circABCA5 promotes the
360 gastric cancer progression by SPI1 mediated IL6/JAK2/STAT3 signaling. *Am J Cancer Res*
361 2023; 13: 602-622.
- 362 [14] COSTA AM, PINTO F, MARTINHO O, OLIVEIRA MJ, JORDAN P et al. Silencing of the
363 tumor suppressor gene WNK2 is associated with upregulation of MMP2 and JNK in
364 gliomas. *Oncotarget* 2015; 6: 1422-1434. <https://doi.org/10.18632/oncotarget.2805>
- 365 [15] XU B, ENGLISH JM, WILSBACHER JL, STIPPEC S, GOLDSMITH EJ et al. WNK1, a
366 novel mammalian serine/threonine protein kinase lacking the catalytic lysine in subdomain
367 II. *J Biol Chem* 2000; 275: 16795-16801. <https://doi.org/10.1074/jbc.275.22.16795>
- 368 [16] VERÍSSIMO F, JORDAN P. WNK kinases, a novel protein kinase subfamily in
369 multi-cellular organisms. *Oncogene* 2001; 20: 5562-5569.
370 <https://doi.org/10.1038/sj.onc.1204726>
- 371 [17] JUN P, HONG C, LAL A, WONG JM, MCDERMOTT MW et al. Epigenetic silencing of
372 the kinase tumor suppressor WNK2 is tumor-type and tumor-grade specific. *Neuro Oncol*
373 2009; 11: 414-422. <https://doi.org/10.1215/15228517-2008-096>
- 374 [18] SIE ZL, LI RY, SAMPURNA BP, HSU PJ, LIU SC et al. WNK1 Kinase Stimulates
375 Angiogenesis to Promote Tumor Growth and Metastasis. *Cancers (Basel)* 2020; 12: 575.
376 <https://doi.org/10.3390/cancers12030575>
- 377 [19] ZHOU SL, ZHOU ZJ, HU ZQ, SONG CL, LUO YJ et al. Genomic sequencing identifies
378 WNK2 as a driver in hepatocellular carcinoma and a risk factor for early recurrence. *J*
379 *Hepatol* 2019; 71: 1152-1163. <https://doi.org/10.1016/j.jhep.2019.07.014>
- 380 [20] WANG Y, WU B, LONG S, LIU Q, LI G. WNK3 promotes the invasiveness of glioma cell
381 lines under hypoxia by inducing the epithelial-to-mesenchymal transition. *Transl Neurosci*
382 2021; 12: 320-329. <https://doi.org/10.1515/tnsci-2020-0180>
- 383 [21] GUERREIRO AS, FATTET S, KULESZA DW, ATAMER A, ELSING AN et al. A sensitized
384 RNA interference screen identifies a novel role for the PI3K p110 γ isoform in
385 medulloblastoma cell proliferation and chemoresistance. *Mol Cancer Res* 2011; 9: 925-935.
386 <https://doi.org/10.1158/1541-7786.MCR-10-0200>
- 387 [22] DENSON LA. Adding fuel to the fire: STAT3 priming of gastric tumorigenesis.
388 *Gastroenterology* 2006; 131: 1342-1344. <https://doi.org/10.1053/j.gastro.2006.08.049>
- 389 [23] JUDD LM, BREDIN K, KALANTZIS A, JENKINS BJ, ERNST M et al. STAT3 activation
390 regulates growth, inflammation, and vascularization in a mouse model of gastric
391 tumorigenesis. *Gastroenterology* 2006; 131: 1073-1085.
392 <https://doi.org/10.1053/j.gastro.2006.07.018>.
- 393 [24] MA Z, SUN Q, ZHANG C, ZHENG Q, LIU Y et al. RHOJ Induces
394 Epithelial-to-Mesenchymal Transition by IL-6/STAT3 to Promote Invasion and Metastasis in
395 Gastric Cancer. *Int J Biol Sci* 2023; 19: 4411-4426. <https://doi.org/10.7150/ijbs.81972>
- 396 [25] THILAKASIRI P, O'KEEFE RN, TO SQ, CHISANGA D, EISSMANN MF et al.
397 Mechanisms of cellular crosstalk in the gastric tumor microenvironment are mediated by
398 YAP1 and STAT3. *Life Sci Alliance* 2024; 7: e202302411.
399 <https://doi.org/10.26508/lsa.202302411>

- 400 [26] SCHUST J, SPERL B, HOLLIS A, MAYER TU, BERG T. Stattic: a small-molecule
401 inhibitor of STAT3 activation and dimerization. *Chem Biol* 2006; 13: 1235-1242.
402 <https://doi.org/10.1016/j.chembiol.2006.09.018>
- 403 [27] BOYD-SHIWARSKI CR, SHIWARSKI DJ, GRIFFITHS SE, BEACHAM RT, NORRELL
404 L et al. WNK kinases sense molecular crowding and rescue cell volume via phase
405 separation. *Cell* 2022; 185: 4488-4506.e20. <https://doi.org/10.1016/j.cell.2022.09.042>
- 406 [28] RODAN AR, JENNY A. WNK Kinases in Development and Disease. *Curr Top Dev Biol*
407 2017; 123 :1-47. <https://doi.org/10.1016/bs.ctdb.2016.08.004>
- 408 [29] MONIZ S, JORDAN P. Emerging roles for WNK kinases in cancer. *Cell Mol Life Sci* 2010;
409 67: 1265-1276. <https://doi.org/10.1007/s00018-010-0261-6>
- 410 [30] WANG F, YAN X, SHI G, ZHANG L, JING X. Loss of WNK1 Suppressed the Malignant
411 Behaviors of Hepatocellular Carcinoma Cells by Promoting Autophagy and Activating
412 AMPK Pathway. *Dis Markers* 2022; 2022: 6831224. <https://doi.org/10.1155/2022/6831224>
- 413 [31] JAYKUMAR AB, JUNG JU, PARIDA PK, DANG TT, WICH Aidit C et al. WNK1
414 Enhances Migration and Invasion in Breast Cancer Models. *Mol Cancer Ther* 2021; 20:
415 1800-1808. <https://doi.org/10.1158/1535-7163.MCT-21-0174>
- 416 [32] JIANG H, CHENG X, LIANG Y, WANG Y, LI Y et al. Aberrant expression of WNK lysine
417 deficient protein kinase 1 is associated with poor prognosis of colon adenocarcinoma. *Ir J*
418 *Med Sci* 2023; 192: 57-64. <https://doi.org/10.1007/s11845-021-02916-5>
- 419 [33] MONIZ S, MARTINHO O, PINTO F, SOUSA B, LOUREIRO C et al. Loss of WNK2
420 expression by promoter gene methylation occurs in adult gliomas and triggers
421 Rac1-mediated tumour cell invasiveness. *Hum Mol Genet* 2013; 22: 84-95.
422 <https://doi.org/10.1093/hmg/dds405>
- 423 [34] FENG DY, ZHENG H, TAN Y, CHENG RX. Effect of phosphorylation of MAPK and Stat3
424 and expression of c-fos and c-jun proteins on hepatocarcinogenesis and their clinical
425 significance. *World J Gastroenterol* 2001; 7: 33-36. <https://doi.org/10.3748/wjg.v7.i1.33>
- 426 [35] MA XT, WANG S, YE YJ, DU RY, CUI ZR et al. Constitutive activation of Stat3 signaling
427 pathway in human colorectal carcinoma. *World J Gastroenterol* 2004; 10: 1569-1573.
428 <https://doi.org/10.3748/wjg.v10.i11.1569>
- 429 [36] LIU M, LI H, ZHANG H, ZHOU H, JIAO T et al. RBMS1 promotes gastric cancer
430 metastasis through autocrine IL-6/JAK2/STAT3 signaling. *Cell Death Dis* 2022; 13: 287.
431 <https://doi.org/10.1038/s41419-022-04747-3>
- 432 [37] LI C, PENG X, PENG Z, YAN B. circBGN accelerates gastric cancer cell proliferation and
433 invasion via activating IL6/STAT3 signaling pathway. *FASEB J* 2022; 36: e22604.
434 <https://doi.org/10.1096/fj.202200957RR>
- 435 [38] THIEM S, EISSMANN MF, ELZER J, JONAS A, PUTOCZKI TL et al. Stomach-Specific
436 Activation of Oncogenic KRAS and STAT3-Dependent Inflammation Cooperatively
437 Promote Gastric Tumorigenesis in a Preclinical Model. *Cancer Res* 2016; 76: 2277-2287.
438 <https://doi.org/10.1158/0008-5472.CAN-15-3089>

439
440 **Figure Legends**

441

442 **Figure 1.** WNK4 was down-regulated in GC cell lines. A) Targeted sequencing results of 100 pairs
443 of gastric cancer samples. Gray rectangles signify different exons, missense mutations (green) and
444 truncation mutations (black) all localized in specific exons. B, C) The expression level of WNK4 in
445 five GC cell lines (AGS, HGC27, MKN28, MKN45, NCIN87) and a normal gastric mucosal cell
446 line (GES-1).

447

448 **Figure 2.** WNK4 overexpression inhibited GC cells proliferation in vitro and in vivo. A) RT-PCR
449 and B) Western-blotting indicated overexpression efficiency of WNK4 in AGS cells. C)
450 Overexpression of WNK4 can effectively inhibited AGS cells proliferation as detected by CCK8
451 assay. D) Colony formation assay revealed that overexpression of WNK4 inhibited the growth of
452 AGS cell lines. E) Subcutaneous graft tumors formed by AGS/oe-WNK4 cells in nude mice were
453 smaller than those generated by controls. F, G) Tumor growth curves and final tumor weights were
454 revealed, respectively, and both metrics had the same trend. H, I) Two groups of tumor specimens
455 were subjected to immunohistochemical detection of Ki67 indicators (magnification $\times 400$). Ki67
456 (green) was assessed by immunofluorescence staining. DAPI was used for nuclear staining (blue).
457 Data were expressed as the mean \pm SD; * $p < 0.05$, ** $p < 0.01$, **** $p < 0.0001$

458

459 **Figure 3.** Knockdown of WNK4 induced GC progression. (A) RT-PCR and (B) Western-blotting
460 indicated knock-down efficiency of WNK4 in MKN45 cells. Knockdown of WNK4 promoted
461 MKN45 cells proliferation were detected by CCK8 assay (C) and Colony formation assay (D). Data
462 were expressed as the mean \pm SD; ** $p < 0.01$, *** $p < 0.001$, **** $p < 0.0001$

463

464 **Figure 4.** The closely association between WNK4 expression and the Jak-STAT3 signaling
465 pathway. A) GSEA analysis of the GC gene expression profiles from the TCGA database showed
466 that low expression of WNK4 was positively correlated with the IL6 Jak STAT3 pathway gene set
467 (NES=1.7, $p < 0.05$). B) Heatmap of the correlation between WNK4 and key genes of the
468 JAK-STAT pathway. Red represents negative correlation; blue represents positive correlation. The
469 larger the correlation r value, the larger the circle. The x represents no significant.

470

471 **Figure 5.** Knockdown of WNK4 activated the STAT3 signaling pathway in GC cells. A) The
472 protein levels of STAT3 and p-STAT3 (Y705) were assessed via Western blot analysis in AGS

473 cells overexpressing WNK4. B) WNK4 knock-down MKN45 cells were also examined for the
474 aforementioned protein levels. C) The effect of Stattic treatment on WNK4 knock-down MKN45
475 cells was evaluated by measuring the protein expression of STAT3 and p-STAT3 (Y705).
476 Functional assays including CCK-8 assay D) and colony formation assay E) demonstrated that
477 Stattic effectively reversed the growth and proliferative capacity induced by WNK4 knockdown in
478 GC cells. F) Schematic representation of WNK4 influencing GC progression through STAT3. Data
479 were expressed as the mean \pm SD; *p < 0.05, ***p < 0.001, ****p < 0.0001

Accepted manuscript

480 **Table1.** Primer sequences for Real-Time qPCR.

Genes	Forward (5'-3')	Reverse (5'-3')
WNK4	TCGGATTGCGAGACTGATG3	GAACGTGGAATGGATAGGG
GAPDH	CGGATTTGGTCGTATTGG	CTCGCTCCTGGAAGATGG

481

Accepted manuscript

Fig. 1 [Download full resolution image](#)

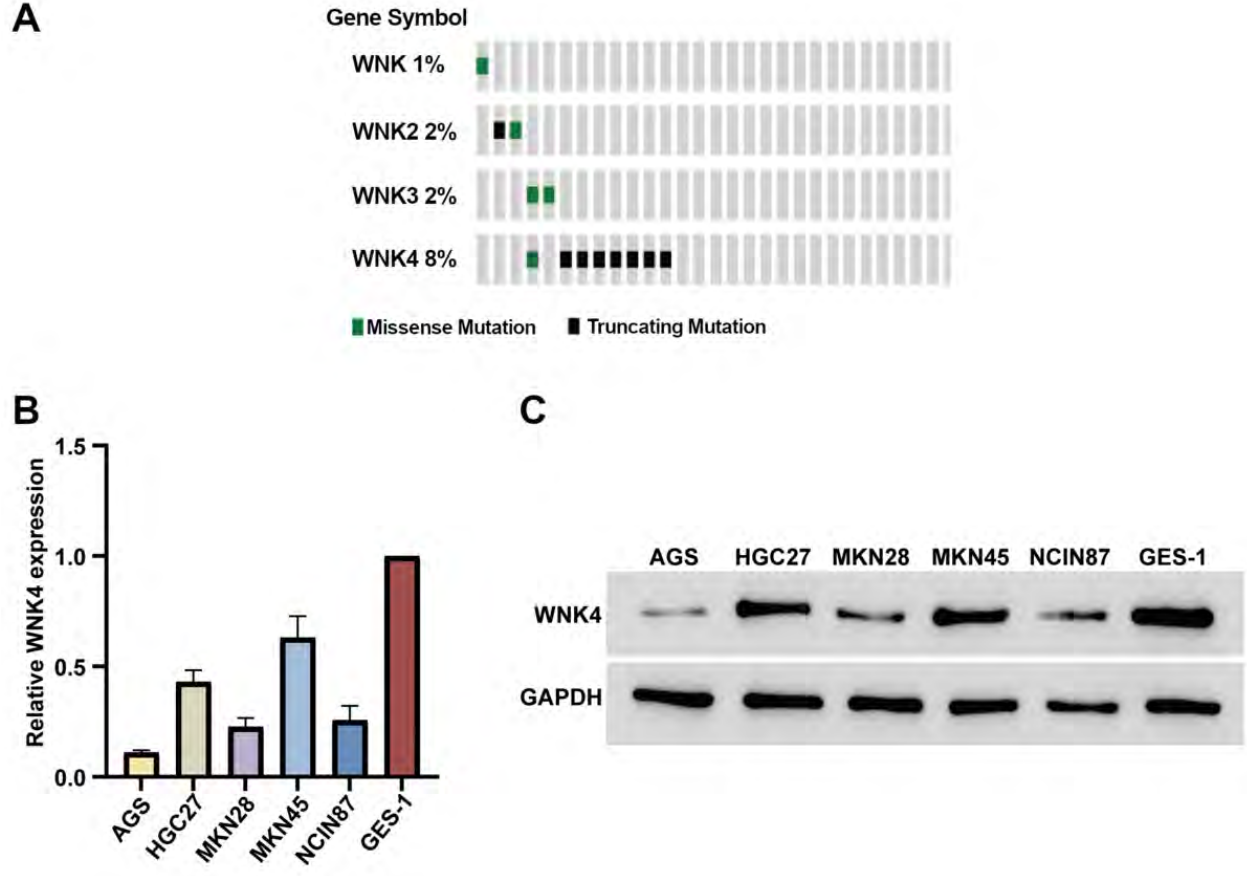


Fig. 2 [Download full resolution image](#)

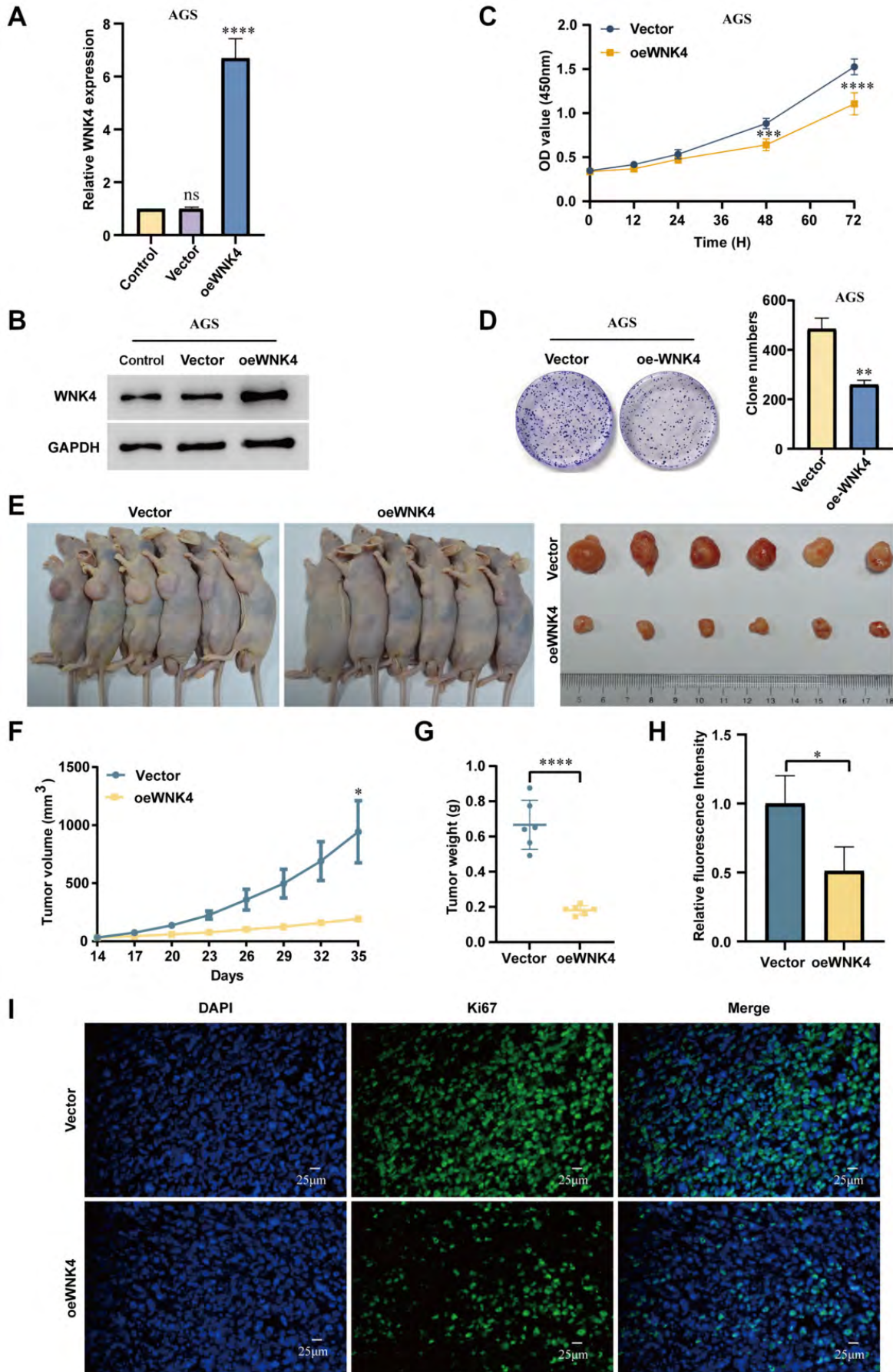


Fig. 3 [Download full resolution image](#)

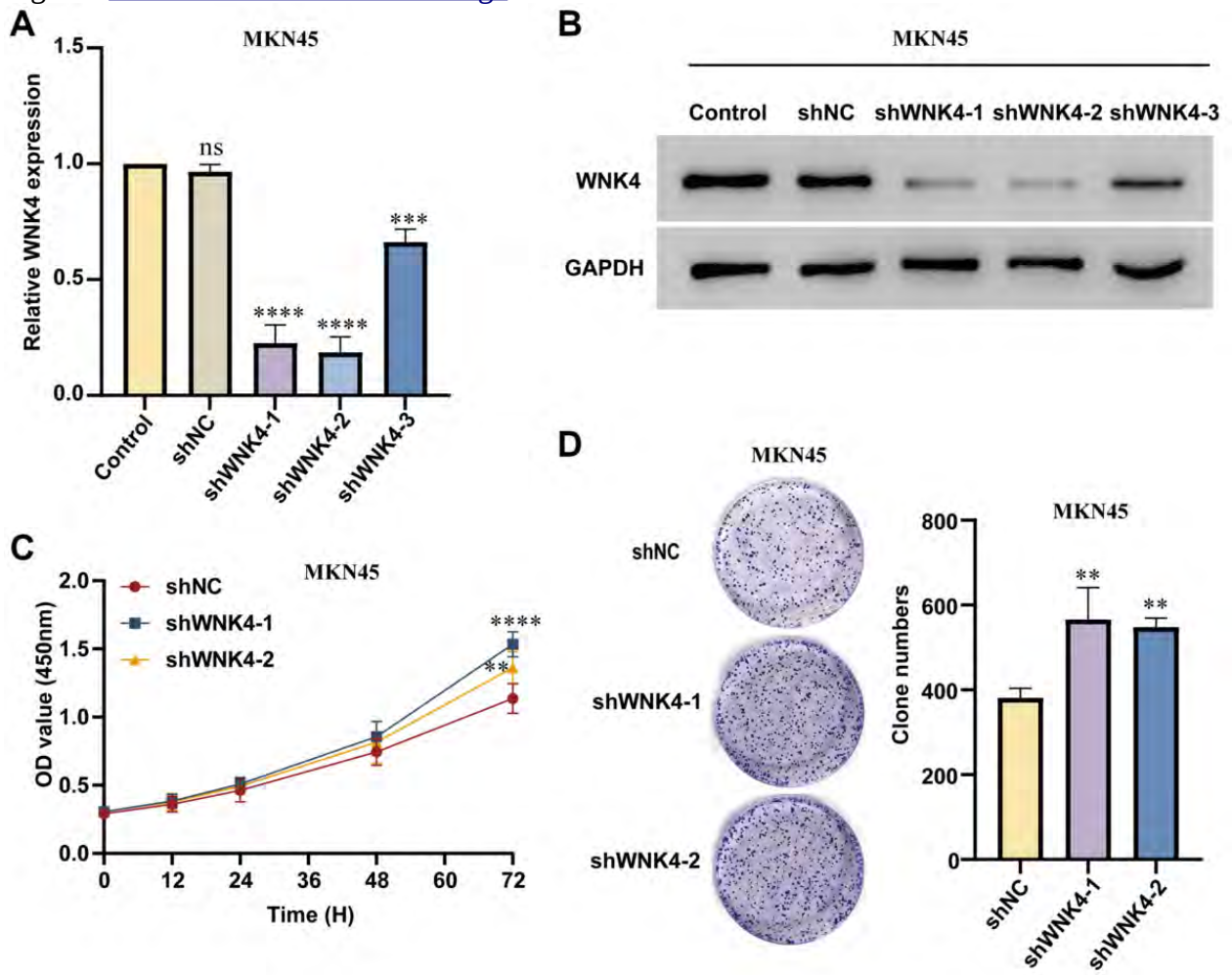
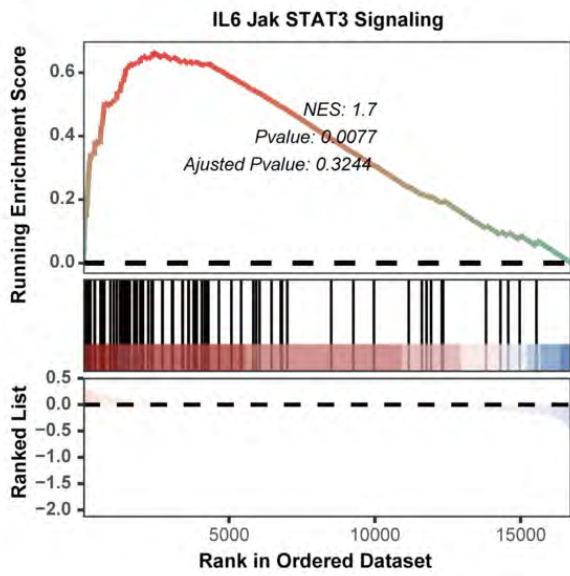


Fig. 4 [Download full resolution image](#)

A



B

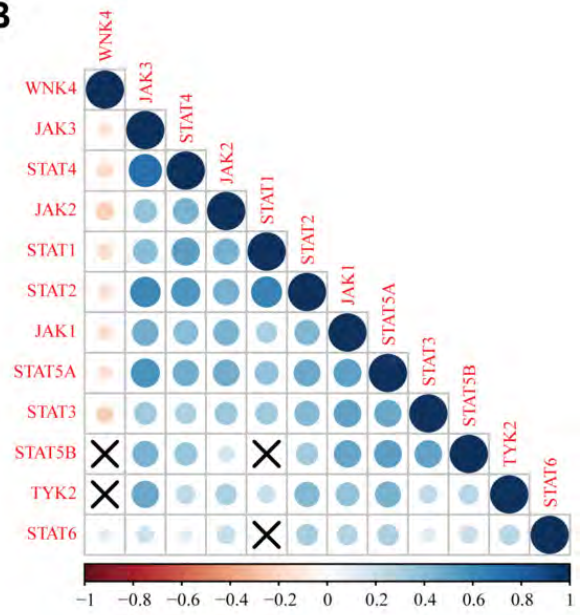


Fig. 5 [Download full resolution image](#)

